

# HEAD SHAPE ESTIMATION USING A PARTICLE FILTER INCLUDING UNKNOWN STATIC PARAMETERS

Catherine Herold<sup>1,2,3,4</sup>, Vincent Despiegel<sup>1,2</sup>, Stéphane Gentric<sup>1,2</sup>,  
Séverine Dubuisson<sup>4</sup> and Isabelle Bloch<sup>1,3</sup>

<sup>1</sup>*Identity & Security Alliance (The Morpho and Télécom ParisTech Research Center), Paris, France*

<sup>2</sup>*Morpho, Safran Group, 11 boulevard Galliéni, Issy-les-Moulineaux, France*

<sup>3</sup>*Télécom ParisTech, CNRS LTCI, Paris, France*

<sup>4</sup>*LIP6, Université Pierre et Marie Curie, 4 place Jussieu, Paris, France*

**Keywords:** Particle Filter, Shape Parameter Estimation, 3D Morphable Model.

**Abstract:** We present a particle filter algorithm to optimize the static shape parameters of a given face observed under multiple views and during time. Our goal is to determine the 3D shape of the head given these observations, by selecting the most suitable deformation parameters. The main idea of our method is to integrate the unknown static parameters in the particle filter hidden state and to filter and modify these parameter values given the recursively incoming observations. We propose here a comparative study of different variants of this approach evaluated on synthetic data. These results show the potential given by this type of particle based methods, which have mainly been presented from a theoretical point of view until now. We conclude with a discussion on the adaptation of these methods to real data sequences.

## 1 INTRODUCTION

Recent improvements in face matching algorithms have led to an increased interest in facial biometry. Nevertheless, for most of these algorithms, a valid frontal view of the head is required to compute the matching score with a frontal reference picture. For Video-Based Face Recognition, obtaining such frontal views is still an issue, especially when the acquisition process has to be fast in an unconstrained scenario. A classical configuration would be a set of cameras situated around a door, acquiring videos of the people passing through to authenticate them “on the fly”. Due to the camera setup and to the “on the fly” scenario, there is no guarantee to have a frontal view directly in any of the input images.

An intermediate step is then required before the matching step, which consists in estimating the pose of the head in each view, extracting its characteristics and recovering a frontal view from the observations. This is usually done by using a three-dimensional head model, which is fitted to the observations by optimizing different parameters (pose, shape, texture). Given this individualized model, it is then possible to synthesize views of the head under any pose. Among all existing head models, the 3D Morphable Model

(3DMM) introduced in (Banz and Vetter, 1999) has been widely used in the last decade. Most of the algorithms used to fit this 3D head model are based on iterative methods, like Levenberg-Marquardt optimization (Romdhani and Vetter, 2005), to minimize a cost function composed of one or several criteria. The main drawback using these methods is their sensitivity to the initialization. Depending on the starting hypothesis, a local minimum can be obtained, which can be far away from the global optimum in case of outliers or noisy observations. As the matching score depends on the quality of the head estimation, it is worthwhile to use all the available observations in the sequence to accurately determine the shape. To our knowledge, only few works have been done on temporal fusion to estimate facial shape parameters. One proposal has been made by (Van Rootsele et al., 2011) and consists in computing the mean of the shape parameters over a set of estimations associated to each timestamp. However, each estimation is done independently at each time, without using previous information.

In order to deal with the problem of local minima and to account for the temporal information, we propose an alternative method to evaluate the best shape parameters: we use a particle filter method which can

take unknown hidden parameters (the shape) into account. The Bayesian context allows for a recursive update of the shape parameter estimation, instead of making independent hypotheses at each frame. Although such methods have already been presented from a theoretical point of view and illustrated with scholar examples (Storvik, 2002; Fearnhead, 2002; Andrieu et al., 2005), only few works have been done in computer vision applications.

After presenting the context of our work and some details on the head model in Section 2, we recall the use of particle filter for dynamic state filtering in Section 3. The extension to methods dealing with static unknown parameters is given in Section 4. We then propose an adaptation of one of them to the temporal head shape estimation issue, which is the main contribution of this paper. As another contribution, in Section 5, we present comparative results of some variations of this method, using a synthetic database for the evaluation. Given the encouraging results with particle filter methods, we conclude this article by mentioning the extension to real data in Section 6.

## 2 CONTEXT AND HEAD MODEL

### 2.1 On the Fly Authentication

The final aim of our application is to authenticate a person walking through a gate or a corridor in an unconstrained scenario. To this aim, we benefit from video streams acquired by a set of cameras situated around the outdoor and directed toward the corridor area. As the faces are observed under non frontal poses, our goal is to compute the corresponding frontal view given the images. Using several images can improve the accuracy of the head reconstruction; indeed, while people are getting close to the cameras, the head is seen under new poses, and some new parts of the head appear. These are useful to complete the previously estimated model and eliminate wrong hypotheses. This is why we propose a method based on the whole stream in this article.

### 2.2 Head Model

As underlined before, our final aim is to estimate as accurately as possible the shape and texture of the observed head to validate the authentication. We employ a 3D head model based on the *3DMM* introduced by (Blaiz and Vetter, 1999). In this paper, we focus on the geometrical part (shape) of the model. This shape model is constructed from a set of  $M$  3D face scans, for which a full correspondence has been

computed (meaning that each 3D vertex  $X_{model}^v$  of a generic model has been associated to the corresponding position  $X^v$  for each face). The set of 3D vertices of one head forms a mesh characterizing the shape. The mean shape  $\bar{S}$  and the main deformation axes  $\{s_i, i \in 1 : M-1\}$  are then computed by a Principal Component Analysis (PCA). Each shape of the space can finally be written as:

$$S = \bar{S} + \sum_{i=1}^{M-1} \theta_i s_i \quad (1)$$

where the shape vector  $\theta = (\theta_1, \dots, \theta_{M-1})$  is distributed with the following probability:

$$p(\theta) \sim e^{-\frac{1}{2} \sum_{i=1}^{M-1} \left(\frac{\theta_i}{\sigma_i}\right)^2} \quad (2)$$

with  $\sigma_i^2, i^h$  eigenvalue of the shape covariance matrix (see (Blaiz and Vetter, 1999) for more details).



Figure 1: Some samples of head appearance for different sets of shape parameters (and a common texture map).

Figure 1 shows some instances created from this 3D shape model, using a fixed texture map. This parametric head shape model has two main advantages. First, the number of unknown parameters determining the shape is widely reduced thanks to PCA. Moreover, by characterizing a face as a linear combination of eigenvectors, we take naturally into account the prior given by the learning database to regularize the solution.

## 3 PARTICLE FILTER FOR DYNAMIC STATE ESTIMATION

We briefly introduce particle filter methods for dynamic state tracking. A complete overview can be found in (Doucet et al., 2000). Let  $x_t$  be the (time-varying) hidden state to estimate, and  $y_t$  an observation. In our case,  $x_t$  corresponds to the 3D head pose at time  $t$  and  $y_t$  to the set of available views at this time. We make the assumption that  $(x_t)_{t=0, \dots, T}$  is a Markov process, meaning that  $x_t$  only depends on the previous state  $x_{t-1}$ . These two states are linked by the prediction equation,  $x_t = f(x_{t-1}, \eta_t)$ , where  $f$  is the transition function and  $\eta_t$  is the noise related to the state dynamics. The observations are linked to the current state by the measurement function  $g$  and an associated measurement noise  $\gamma_t$ :  $y_t = g(x_t, \gamma_t)$ .

Tracking processes are often expressed in a Bayesian framework (Isard and Blake, 1998). In this context, the aim is to estimate the density of the current state given all previous and current observations, written  $p(x_t|y_{0:t})$ . This probability is computed in a recursive way, and given by:

$$p(x_t|y_{0:t}) \propto \underbrace{p(y_t|x_t)}_{\text{likelihood}} \int_{\mathcal{X}} \underbrace{p(x_t|x_{t-1})}_{\text{state dynamics}} \underbrace{p(x_{t-1}|y_{0:t-1})}_{\text{previous density}} dx_{t-1}, \quad (3)$$

where  $\mathcal{X}$  is the dynamic state space.

When the transition and the measurement functions are linear, and  $\eta_t$  and  $\gamma_t$  are Gaussian additive noises, the probability can be computed in an analytical way with the Kalman filter. To handle other cases, particle filters have been proposed in the 1990's. In this context, the posterior  $p(x_t|y_{0:t})$  is estimated by a sequential Monte-Carlo method with a set of  $N$  weighted particles. Each particle  $x_t^{(i)}$  represents a possible realization of the state  $x_t$ , and its weight  $w_t^{(i)}$  evaluates its consistency given the observations. The probability  $p(x_t|y_{0:t})$  is then approximated by  $p(x_t|y_{0:t}) \approx \sum_{i=1}^N w_t^{(i)} \delta(x_t^{(i)} - x_t)$ . Given the initial particles set  $\{(x_0^{(i)}, w_0^{(i)}), i = 1 : N\}$ , the posterior density is recursively estimated at each timestamp using three steps. First, during the prediction step, each particle  $x_{t-1}^{(i)}$  moves from time  $t-1$  to time  $t$  given the probability  $p(x_t|x_{t-1})$  associated with the system dynamics. The weights  $w_t^{(i)}$  are then updated according to the current observation  $y_t$ , using  $p(y_t|x_t^{(i)})$ . Finally, a resampling is performed if the particle weights are too spread.

The particle filter outcome depends on the number of particles used to approximate the density over the hidden state space. Indeed, if too few particles are sampled in the space, the subregions containing the most probable parameters are not necessarily visited, and the filter remains uninformative. When increasing the size of the particle state space by including new parameters, it is therefore necessary to adapt the number of particles.

## 4 PARTICLE FILTER WITH UNKNOWN PARAMETERS

At this stage, we can point out that the head shape (which is unknown at the beginning of the sequence) influences the pose evaluation. Indeed, if we estimate the pose of a distorted head using the mean shape model, a perfect fitting will probably not be possible,

and the shape difference will be balanced by a pose correction. For instance, for someone having a thin head, ears are close to the eyes, which is not the case for the mean model used for the pose estimation. The yaw angle may then be overestimated to reduce the distance between the ear and the eye projections.

Moreover, for biometric applications, we are not only interested in these pose parameters at each time, but also in the shape parameters explaining the whole set of observations, in order to associate the correct pixel with each 3D vertex, and generate an accurate frontal view at the end of the process. This issue is the subject of this section, presenting a short review of particle filter algorithms when unknown static parameters have to be taken into account and estimated. We especially develop how these methods can be adapted to estimate the unknown head shape parameters, given a set of observations acquired recursively in time.

### 4.1 Particle Filter for Static Parameter Estimation

Let  $\theta$  be the vector of dimension  $s_\theta$  containing all unknown static shape parameters, and  $\Theta$  the associated parameter space. We can rewrite the particle filter equations when  $\theta$  has to be taken into account (and eventually evaluated):

$$\begin{cases} x_t = f(x_{t-1}, \eta_t) \\ y_t = g(x_t, \theta, \gamma_t) = g_\theta(x_t, \gamma_t) \end{cases} \quad (4)$$

where  $x_t$  is the time-varying head pose (*i.e.* the 3D head center position and the head orientation).  $\theta$  does not appear in the first equation as the head shape does not influence the pose dynamics. However, the second equation depends on  $\theta$ , as the shape parameters modify each 3D head vertex position, and therefore its associated projection in the images.

In order to account for the presence of unknown parameters, several methods have already been explored, mostly theoretically. In (Kantas et al., 2009), the authors list a set of existing methods to estimate static parameters using particle filters. One can separate the offline methods, which use simultaneously all the observations to make a unique global optimization, from online methods, which update recursively the parameter estimation when new observations become available. We consider only this second case, adapted to our application, where each observation  $(y_t, t = 1, \dots, T)$  corresponds to a frame of a video stream. The aim is to recursively compute an estimation  $\theta^*$  each time a new observation is available.

Among online approaches, particle filter methods with unknown static parameters can proceed in two different ways:

1. compute an estimation  $\theta^*$  by expectation-maximization or gradient descent methods. The optimization returns directly a unique value for  $\theta^*$ . This method aims at maximizing the marginal likelihood  $p_\theta(y_{1:t})$ , thanks to a deterministic or stochastic gradient descent method:

$$\theta_t = \theta_{t-1} + \gamma_t \nabla_{\theta} \log p_{\theta_{1:t-1}}(y_t | y_{1:t-1}) \quad (5)$$

using Monte-Carlo techniques to approximate the score  $\nabla \log p_{\theta_{1:t-1}}(y_t | y_{1:t-1})$ .

2. integrate the static parameters in the hidden state, thus increasing the state dimension. Monte-Carlo methods are then used to estimate the joint density  $p(\theta, x_{1:t} | y_{1:t})$  over the mixed state, which can be marginalized with respect to the dynamic state  $x_{1:t}$ . A specific value of  $\theta^*$  can be obtained from this approximated density, as the best particle state or the mean over the particle set.

Due to the sensitivity to initialization of gradient algorithms (Kantas et al., 2009), we favor the second way of estimating  $\theta^*$ , which integrates the static parameters in the particle state. Nevertheless, some types of artificial moves introduced in the coming part may create a bias on the estimation accuracy.

## 4.2 Introducing Unknown Parameters in the State Space

Several authors (Storvik, 2002; Fearnhead, 2002; Minvielle et al., 2010) suggest to integrate the static parameters in the particle state. The complete state to evaluate becomes the concatenation  $\xi = \{x, \theta\} \in \mathcal{X} \times \Theta$ , where  $x$  is the head pose and  $\theta$  the static parameters (the shape weighting factors in Equation (1)). Each particle will then represent both a shape parameter hypothesis and an associated pose.

From the particle filter defined over the mixed state, one can infer the distribution  $p(\theta | y_{1:t})$  by integrating on the dynamic state space  $\mathcal{X}^t$ :

$$p(\theta | y_{1:t}) = \int_{\mathcal{X}^t} p(x_{1:t}, \theta | y_{1:t}) dx_{1:t}. \quad (6)$$

As underlined in several papers, the integration of static parameters in the hidden state can lead to impoverishment issues if no dynamics are used in the evolution process (although by definition, the static parameters do not change with time). Indeed, due to resampling steps, most of the initial values will gradually disappear, leading to a restrictive set of possible values. Moreover, only the initially sampled parameters can be evaluated and selected. It is therefore required to include particle state moves between two evaluations, despite their static aspect, in order to allow a better shape space exploration. This can be

done with artificial and systematic dynamics, smart diversification parametrized by the particle weights or specific sampling procedures. We present the various moves tested in our case.

**Artificial Dynamics.** As in (Minvielle et al., 2010), we apply a fixed and automatic artificial dynamic on the static parameters for all particles. Given a particle  $(x_{t-1}^{(i)}, \theta_{t-1}^{(i)}, w_{t-1}^{(i)})$ , this artificial dynamic will lead to the new shape parameters at time  $t$ :

$$\theta_t^{(i)} = \theta_{t-1}^{(i)} + n_\theta, \quad (7)$$

where  $n_\theta$  is a Gaussian noise with zero mean.

An intuitive idea is to use the particle weight to adapt the noise applied on the static parameters. Indeed, if a particle has a small weight, the current parameters might be distant from the true ones, this is why it is useful to strongly modify them in order to explore another space area of the shape parameters. Conversely, if the current weight is high, it is interesting to look around the current state to search for a possible higher value (local optimization). To take this into account, we propose a modified version of the previous artificial move algorithm by making the noise  $n_\theta$  in Equation (7) dependent on the particle weight  $w_{t-1}^{(i)}$  to improve the particle moves in the static space. More specifically, the noise variance is inversely proportional to the weight.

**MCMC Moves.** In (Fearnhead, 2002), the particle diversity in the static parameter space is obtained thanks to a step of MCMC (Monte Carlo Markov Chain) process. This step allows conditional particle moves in subspaces with high probability, by adding a Gaussian noise to the static state (this contrasts with the resampling step, which keeps each sampled particle identical to the original one). This idea, called *Resample-Move algorithm*, has been introduced in (Gilks and Berzuini, 2001). The process is the following: at each timestamp  $t$ , a MCMC move is generated given a kernel  $K_t(x'_{1:t}, \theta' | x_{1:t}, \theta)$ , having  $p(x_{1:t}, \theta | y_{1:t})$  as invariant distribution. This move can be applied on the static parameters  $\theta$  only:

$$K_t(x'_{1:t}, \theta' | x_{1:t}, \theta) = \delta_{x_{1:t}}(x'_{1:t}) p(\theta' | y_{1:t}, x_{1:t}) \quad (8)$$

and can be obtained with a Gibbs sampler or with a two-step Metropolis-Hastings (MH) algorithm:

1. Sample randomly a candidate  $\theta'_t \sim p(\theta'_t | \theta_t)$
2. Sample  $v \sim \mathcal{U}_{[0,1]}$ .

$$\text{If } v \leq \min \left( 1, \frac{p(y_{1:t} | x_{1:t}, \theta')}{p(y_{1:t} | x_{1:t}, \theta)} \right) \quad (9)$$



the move towards  $\theta'$  is accepted; otherwise,  $\theta$  is kept.

We can underline here that it can be costly to apply this formula directly. Indeed, even if we only change the static parameters, this modification requires to keep in memory all previous observations and to recompute all the likelihood values at previous times, which is computationally more and more expensive. This is why we introduce a period  $\Delta T$ , which characterizes the number of frames used for the MCMC validation. The move validation depends then on:

$$v \leq \min \left( 1, \frac{p(y_{t-\Delta T:t} | x_{t-\Delta T:t}, \theta')}{p(y_{t-\Delta T:t} | x_{t-\Delta T:t}, \theta)} \right), \quad (10)$$

with  $\Delta T = 0$  if we only use the current observations.

The Bayesian method including a MCMC sampling step has the advantage to keep the probability  $p(\theta | y_{0:t})$  invariant, unlike the basic method which introduces a bias due to the Gaussian noise added on static parameters. Nevertheless, these methods need more evaluation steps (one more per particle during the move validation), and are not robust when  $t \gg 1$ . As in our case,  $t$  is limited by the number of available frames (about 20) and as we only have a few parameters to estimate, we are in the conditions underlined in (Kantas et al., 2009) for which this method is suitable.

As in the case of systematic Gaussian noise addition on the static parameters, the MH-sampling step only allows a local diversification of the static parameters. Another option we propose is to make a global sampling step from the current approximation  $p(\theta | y_{0:n})$  (or a prior on the static parameters), independently of the particle current state  $(x_t^{(i)}, \theta_t^{(i)})$ . Intuitively, this means that any move is allowed, as long as the likelihood is improved with the new set of parameters. This helps the particles to get out from local maxima when more likely states exist.

### 4.3 Likelihood Functions

When estimating the head shape parameters, there is a specific difficulty due to the non-trivial relation between the unknown shape and pose on the one hand, and the corresponding observation on the other hand. The function  $g$  in Equation (4), which can be related to the update step, contains actually the head model deformation, its pose transformation, and finally the projection function to obtain the images. Special attention should be paid to the likelihood functions used at this point.

We describe here more precisely the functions used in the proposed algorithm for face shape estimations. During the observation step, the particle weights are updated according to the particle agreement with the current observations, using three different likelihood functions:

- one is derived from a distance between the 2D feature point inputs and their retroprojection in each view given the particle pose and shape parameters (Figure 2(a)).
- the second one is derived from the direction similarity between the gradients of the internal edges (Figure 2(b)) projected from the model, and the observed gradients at the same image location.
- the third one is derived from the silhouette similarity (Figure 2(c)) and is computed in the same way as the internal edge score.

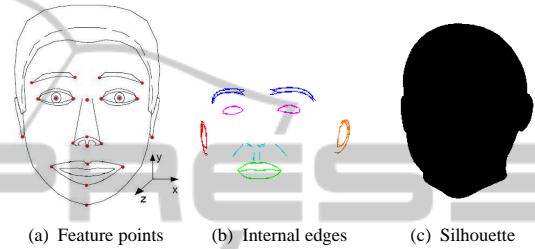


Figure 2: Features used for the likelihood computation.

Under independence hypotheses on the edge and feature point detectors, the three probabilities derived from these scores can be multiplied to obtain the global likelihood. Algorithm 1 summarizes the global process of parameter estimation.

---

**Algorithm 1:** Static shape parameter estimation with a particle filter.

---

Sample the shape parameters  $\theta$  from a prior Gaussian distribution to initialize the set of particles  $\{(x_0^{(i)}, \theta_0^{(i)}, w_0^{(i)} = 1/N), i = 1 : N\}$

**for**  $f = 1 \rightarrow N_{frames}$  **do**

Input: noisy 2D feature point positions.

Mean shape model fitting to estimate the initial pose  $x_t^0$  using the method by (Umeyama, 1991).

**for**  $i = 1 \rightarrow N$  **do**

- Sample around the estimated pose:

$$x_t^{(i)} = x_t^0 + n_x, \text{ with } n_x \sim N(0, \Sigma_x). \quad (11)$$

- (Optional) Sample around the previous shape parameters:  $\theta_t^{(i)} = \theta_{t-1}^{(i)} + n_\theta$ , with  $n_\theta \sim N(0, \Sigma_\theta)$ .

- Update the weight with the likelihood

$$p(y_t | x_t^{(i)}, \theta_t^{(i)}): w_t^{(i)} \propto w_{t-1}^{(i)} p(y_t | x_t^{(i)}, \theta_t^{(i)}).$$

**end for**

Resampling

**for**  $i = 1 \rightarrow N$  **do**

(Optional) Apply a MCMC move

**end for**

**end for**

---

## 5 RESULTS ON SIMULATED DATA

### 5.1 Data Generation and Evaluation

To evaluate the different particle filter versions presented in Section 4.2 (systematic noise addition, possibly parametrized by the weight and MCMC with local or global sampling), we concentrate our work on synthetic data in order to benefit from the ground truth values for the pose and the shape parameters.

The test faces are generated with two shape parameters ( $s_\theta = 2$ ) sampled from the standard normal law, the pose during the sequence is similar to the one in real sequences, and the images are obtained with the same calibration parameters as in our acquisition system.

We applied the different particle filter methods on noisy data ( $\sigma = 2$  pixels for the feature point inputs), to simulate detector answers on real data. This leads to an approximate pose initialization and to a score function disturbed by this noise. The proposed experimental analysis is novel and provides a deeper insight on the different particle filter methods of Section 4 applied on face image sequences. It presents the possibilities offered by particle methods, when complex transformations are involved between the observations (the image sequences) and the hidden state (pose and shape parameters).

### 5.2 Parameter Convergence

#### 5.2.1 With Known Dynamic State

In a first experiment, we check the convergence of the particle static states towards the correct shape parameters when the head pose is known. In this case, the only unknowns are the two static shape parameters. The best particle and the filter mean and variance are plotted for one sequence in Figure 3. They can be compared to the ground truth values plotted in green solid line (GT). We can observe that the mean of the filter converges towards the real parameters, and that the variance decreases at the beginning of the sequence before stabilizing. In this example, even if few particles are sampled around the true first parameter at the initialization step, the whole set of particles moves towards this value over the sequence.

#### 5.2.2 With Unknown Dynamic State

To simulate real data issues, in which the pose is not known, we now integrate the hidden dynamic state  $x_t$  in the estimation process. Besides the two unknown

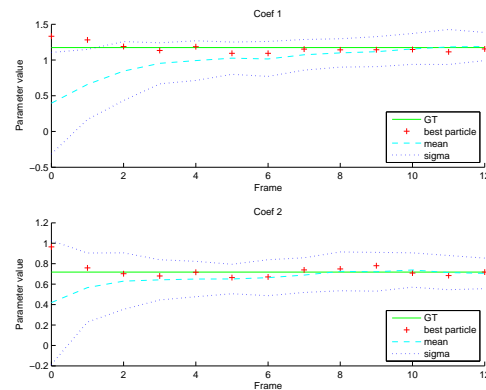


Figure 3: Evolution of the filter static parameters when the pose is known. 100 particles are used, artificial moves are Gaussian noises with fixed covariance.

shape parameters already estimated before, there are now six more time-varying unknowns, corresponding to the 3D position and the 3 rotation angles. This explains why we use more particles in the coming experiments, still conducted on synthetic data.

**Robustness to the Pose Error.** We initially evaluate the algorithm robustness to an initial pose error. To this aim, we launch the algorithm using various input poses as initial pose estimation  $x_t^0$  in Equation (11): first the true pose, before adding various yaw angle errors (2, 4, 6, 8 and 10 degrees). Particle poses are then sampled around this modified pose input. Figure 4 illustrates the results for these replays, and shows that below 8 degree error on the initial yaw estimation, the convergence results are comparable. For higher errors, too few particles are sampled around the true pose which makes the convergence less probable. An higher dynamic noise  $n_x$  in Equation (11), associated with more particles can be considered if larger pose errors are expected. However, in our study, the initial pose remains generally below the convergence threshold. Further study on robustness to simultaneous position and angle errors will help to optimize these two parameters.

In fact, the true pose is not available, the pose is therefore initialized as follows for the rest of the evaluation: the input feature point detections are used to fit the mean model, and the resulting pose  $x_t^0$  is used to initialize the particle dynamic states (Algorithm 1).

**Gaussian Noise on the Static Parameters.** Figure 5 shows the filter evolution for the same sequence as in Figure 3, but with unknown pose parameters. The artificial dynamic is a Gaussian noise with fixed covariance for all particles. We can observe that the deviation is larger than in the previous case. As the pose has to be estimated simultaneously, the particles hav-

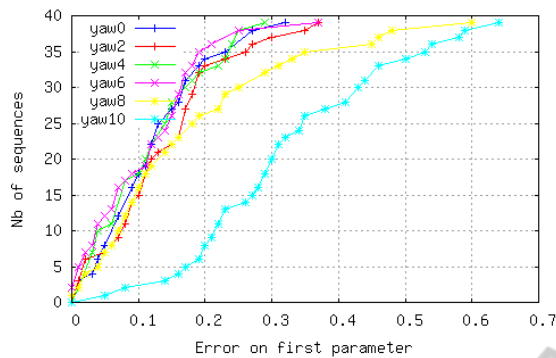


Figure 4: Robustness to the initial yaw angle error. From 0 degree (yaw0) to 10 (yaw10).

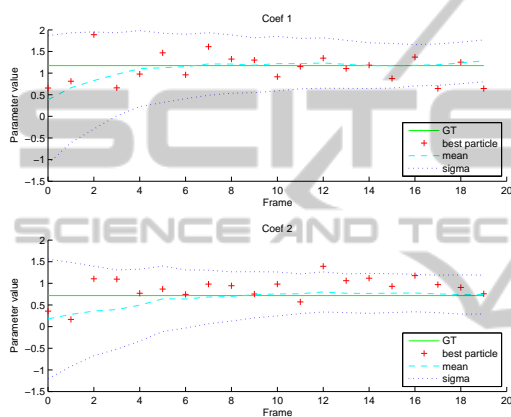


Figure 5: Evolution of the filter static parameters when the pose is unknown. 2500 particles, artificial moves are Gaussian noises with fixed covariance.

ing correct poses but wrong shape parameters might be weighted as the ones having the inverse configuration. The shape parameter filtering takes therefore more time to converge.

**Adaptive Noise.** Figure 6 shows some convergence results with 2500 particles, given input data without noise.

Adding a noise of 2 pixels on the feature point positions, we get the results presented in Figure 7. Despite this observation alteration, the filter means for the static parameters are close to the true values.

**MCMC Moves.** this method uses a validation step before modifying the static parameters sampled for a particle. We evaluate two types of sampling: local sampling around the current value, and global sampling given the Gaussian prior. The move is only applied on the static shape parameters, thus optimizing the shape at a fixed pose. This step implies a new likelihood computation, that should theoretically be done on the whole set of observations  $y_0, \dots, y_t$ . In this case, the validity of the pose  $x_0^{(i)}, \dots, x_{t-1}^{(i)}$  is ques-

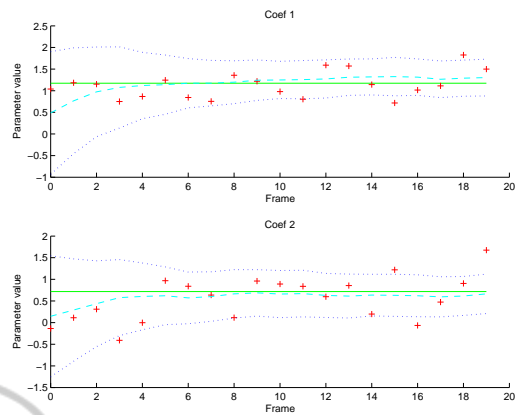


Figure 6: Evolution of the filter static parameters, when the pose is unknown. No noise is added on the input feature points. Artificial moves are Gaussian noises with adaptive covariance.

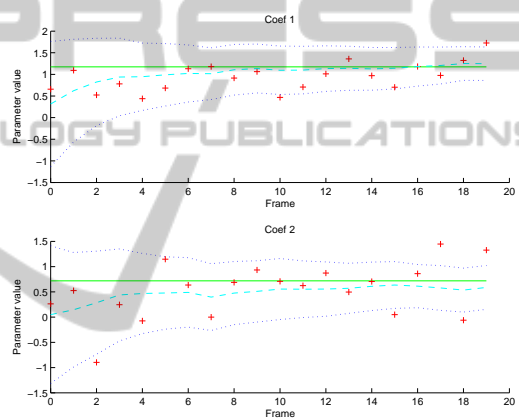


Figure 7: Evolution of the filter static parameters when the pose is unknown. Noise is added on the input feature points. 2500 particles, artificial moves are Gaussian noises with adaptive covariance.

tionable and may be wrong. By using these pose parameters, the shape values which have been validated with these poses will be preferred. This is why we use  $\Delta_T = 0$ , meaning that only the current view is used to compute the move acceptance. Figure 8 shows the filter evolution for the two types of sampling methods, which lead to similar results.

**Methods Comparison.** Let  $\theta_{GT}^1$  be the true value of the first shape parameter and  $\theta_{eval}^1$  the mean value over the particle states. To evaluate the different methods, we measure the error  $\epsilon = |\theta_{eval}^1 - \theta_{GT}^1|$  for our 39 synthetic sequences on the last frame of the sequence. Figure 9 shows that all methods provide globally similar results.

Curves 3, 4 and 5 present results when a systematic noise is added at each time on the static parameters. Using an adaptive noise (curve 4) instead of a

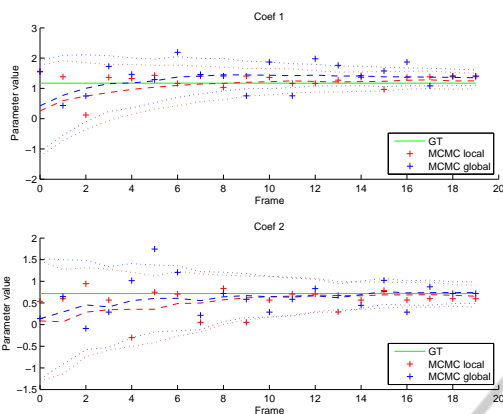


Figure 8: Evolution of the filter static parameters when the pose is unknown. 2500 particles, MCMC moves.

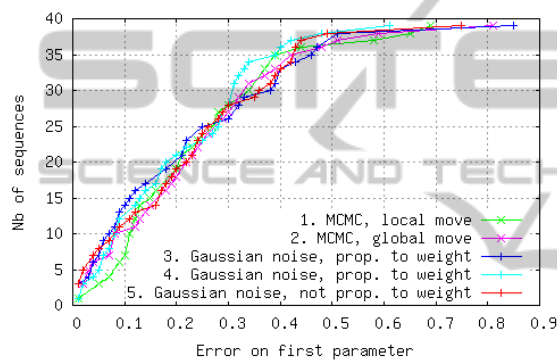


Figure 9: Cumulative error distribution. The prior on  $\theta$  is  $(m = 0, \sigma = 1.7)$  for curves 1, 2, 4, 5 and  $(m = 0, \sigma = 1.0)$  for curve 3.

fixed noise (curve 5) results in more accuracy thanks to a better state space exploration. We can also notice that the prior sampling on the parameter space (normal law with parameters  $(m = 0, \sigma = 1.0)$  for curve 3,  $(m = 0, \sigma = 1.7)$  for curve 4) influences slightly the curves: with a wide distribution, it becomes easier to reach large values of the parameters, as more particles will then be sampled around the true value. Conversely, for narrow initial sampling, the particles are concentrated in a smaller area, which leads to more accurate results when the parameters are close to zero. This explains why curve 3 is above the others for small errors. The highest error is around 0.6 for the wide sampling (curve 4), against 0.85 using standard normal law (curve 5). These values can be compared to the interval covered by all  $\theta_{GT}^1$  of our database,  $[-2.97; 2.10]$ , sampled from the standard normal law. Using the weight adaptive noise method and a large deviation for the initial parameter sampling, 87% of replays verify  $\varepsilon \leq 0.34$  (6.7% of the interval width).

Although MCMC moves involve a validation step using the Metropolis-Hastings algorithm, the two

evaluated methods (curves 1 and 2) do not outperform the previous ones, based on a systematic noise addition. Automatic noise methods may therefore be preferred since the other methods do not provide significant accuracy improvements despite their higher computational cost.

**Failure Cases.** For some sequences, the true values are never reached during the filtering process. The explanation is twofold. First, it can be due to the model prior used to initialize the static parameter particles. When the true parameters are very different from zero ( $|\theta_i| \geq 1$ , for  $i = 1 : s_\theta$ ), the probability to sample these true values becomes low, and the static parameter moves do not always compensate for the initialization (Figure 10(a)). Secondly, the 3D pose can be poorly estimated, for instance with very noisy detections. As all particles are sampled around it, no particle has a pose close to the true one. In this case, the shape optimization will not succeed, as a good pose approximation is required to estimate the parameters.

These two issues are sometimes linked. Indeed, the mean head model fitting used to obtain an initial pose estimation is worse when the model is highly deformed (Figure 10(b)). In this case, there are few particles both in the appropriate pose and shape subspaces. A solution could be to evaluate the initial pose with each particle shape model, at the cost of  $N$  pose fittings.

## 6 EXTENSION TO REAL DATA

The previous results have been computed over a set of synthetic sequences to evaluate the behavior of different particle filter variants. Before estimating the head shape parameters on real data by using a particle filter including these unknowns in the hidden state, some issues related to the likelihood validity and to the head model have to be considered.

### 6.1 Adaptation of Likelihood Functions

**Likelihood Issues on Real Data.** Several issues have to be considered when working with real data. First, due to the non frontal poses, some feature points may be badly or not detected. Besides, the lighting conditions can induce shadows (Fig.11(b)), creating unwanted gradients which can match with edges or silhouette projection. This is also the case with occlusions generated by glasses, beards, hair... (Fig.11(a) and 11(c)). Moreover, these occlusions can lead to false or missed feature point detections. Finally, as the background can be similar to the skin color, the



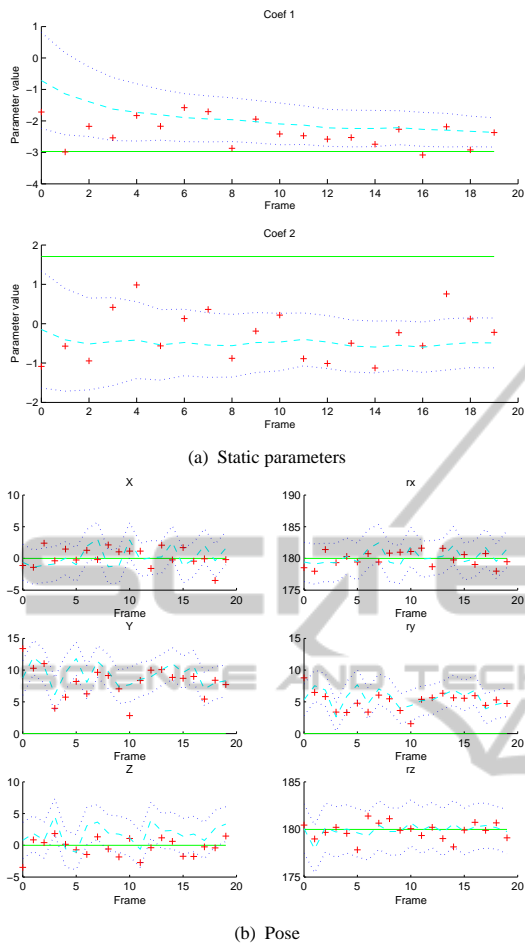


Figure 10: Evolution of the particle filter with unknown pose and noisy observations. 2500 particles are used, artificial moves are Gaussian noise with adaptive covariance.

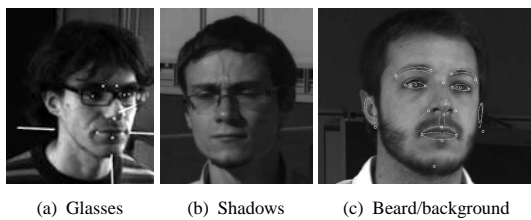


Figure 11: Likelihood issues on real data.

silhouette gradient is not always observable, as shown in Fig.11(c).

**Criteria Revision.** The feature point detectors can lead to outliers, which have to be handled when estimating the initial pose. Having a set of detections associated with a feature point in multiple views, it is possible to check its 3D coherence, and thus to detect potential outliers. Another solution is to use a RANSAC procedure when estimating the pose, to

only keep coherent detections given the model. When computing the particle likelihood, it is also necessary to use a robust distance score, in order to limit the influence of these false detections.

To compute the edge criteria on real data, additional information can be taken into account. As we can give more confidence to edges with high magnitude, we can weight the orientation similarity by the gradient norm.

For real data, the internal edge likelihood is less picky than for synthetic data. As the contours are not properly defined on real images, the corresponding likelihood function presents several optima. Indeed, various particles can have similar weight on internal edges and feature point criteria, but can be discriminated by the silhouette criterion (Figure 12). More importance can be given to the silhouette criterion to improve the selection during the resampling step.

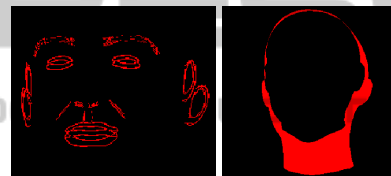


Figure 12: Features for shapes  $\theta_a(-1.3;1.4)$ ,  $\theta_b(1.6;-0.8)$ .

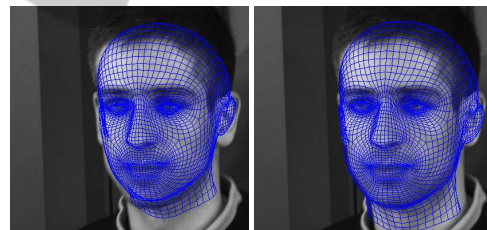


Figure 13: Mesh projection examples.

Figure 13 illustrates the fitting gain between the initial mesh and the best particle mesh after the observation update. The mean mesh on the left does not perfectly fit the silhouette and the internal edges, which lead to a lower score than the one of the right mesh, which corresponds to the best particle sampled at this stage. This particle mesh matches especially better than the initial mesh on the silhouette observation, which shows again the importance of this criterion. This also illustrates the feasibility and the interest of the proposed approach on real data.

In the future, we will especially work on different ways to perform the fusion between the criteria. One advantage using particle filter is the possibility to maintain several hypotheses through the sequence. When no particle gets a high score on all criteria, the

ones with good scores for one or two criteria will be kept, until new data can be used to make the selection.

## 6.2 True Solution Approximation

As we generated our evaluation dataset from the shape model, the solution belongs to the shape space. However, this is not the case for real faces. Our shape model covers actually only a subspace of the head shape space, so there is not necessarily a solution such that all 3D estimated vertex positions correspond to the true ones. We search therefore the best shape approximation in the subspace, for instance the one minimizing the distance between two meshes. There might be several set of parameters verifying the minimum reachable likelihood score. These multi-hypotheses can easily be characterized by particle filters, through multi-modal density. In this case, a preliminary step of mode detection is necessary to extract the parameters, instead of computing the mean over the whole distribution.

For future evaluation on real data, we do not benefit from the true coefficients for an observed head. An evaluation of the algorithm by shape parameter comparison will neither be possible, nor meaningful. Beyond visual control, new metrics need to be designed, as for instance a measure between two three-dimensional meshes (assuming that the true shape is known, using 3D scans for instance). Evaluation can also be performed by comparing manual annotations of feature points, edges and silhouettes, with the ones projected from the estimated head shape and poses.

## 7 CONCLUSIONS

We introduced in this paper a new method to optimize the shape parameters of a head seen in multiple video streams. Instead of using common gradient descent methods on each frame, we propose to use a particle filter algorithm including static parameters in the hidden state, resulting in a probability approximation over the shape space. An advantage of this method is its ability to update the estimation when new observations are available, thus increasing the estimation accuracy recursively. Several variants of this method have been evaluated, presenting similar accuracy results. Given its low computation requirement and its results, a systematic noise addition dependent on the particle weight is recommended as a good compromise. Finally we discussed the potential application of the proposed particle filter including static parameters on real data, by highlighting the problems that can be anticipated and proposing solutions to solve

them. Promising results have already been obtained, and future work aims at exploring these solutions in depth.

## REFERENCES

- Andrieu, C., Doucet, A., and Tadic, V. B. (2005). On-line parameter estimation in general state-space models. *Proc. IEEE Conf. on Decision and Control*, pages 332–337.
- Blanz, V. and Vetter, T. (1999). A Morphable Model for the Synthesis of 3D Faces. In *SIGGRAPH*, pages 187–194.
- Doucet, A., Godsill, S., and Andrieu, C. (2000). On Sequential Monte Carlo Sampling Methods for Bayesian Filtering. *Statistics And Computing*, 10(3):197–208.
- Fearnhead, P. (2002). MCMC, Sufficient Statistics and Particle Filters. *Journal of Computational and Graphical Statistics*, 11(4):848–862.
- Gilks, W. R. and Berzuini, C. (2001). Following a Moving Target - Monte Carlo Inference for Dynamic Bayesian Models. *Journal of the Royal Statistical Society: Series B (Statistical Methodology)*, 63(1):127–146.
- Isard, M. and Blake, A. (1998). Condensation – Conditional Density Propagation for Visual Tracking. *International Journal of Computer Vision*, 29(1):5–28.
- Kantas, N., Doucet, A., Singh, S. S., and Maciejowski, J. M. (2009). An Overview of Sequential Monte Carlo Methods for Parameter Estimation in General State-Space Models. *Proc. IFAC System Identification SysId Meeting*, (MI).
- Minvielle, P., Doucet, A., Marrs, A., and Maskell, S. (2010). A Bayesian Approach to Joint Tracking and Identification of Geometric Shapes in Video Sequences. *Image and Vision Computing*, 28(1):111–123.
- Romdhani, S. and Vetter, T. (2005). Estimating 3D Shape and Texture using Pixel Intensity, Edges, Specular Highlights, Texture Constraints and a Prior. In *Proc. Computer Vision and Pattern Recognition*, pages 986–993.
- Storvik, G. (2002). Particle Filters for State-Space Models with the Presence of Unknown Static Parameters. *IEEE Trans. on Signal Processing*, 50(2):281–289.
- Umeyama, S. (1991). Least-Squares Estimation of Transformation Parameters Between Two Point Patterns. *IEEE Trans. on Pattern Analysis and Machine Intelligence*, 13(4):376–380.
- Van Rootsele, R. T. A., Spreeuwiers, L. J., and Veldhuis, R. N. J. (2011). Application of 3D Morphable Models to Faces in Video Images. In *Symp. on Information Theory in the Benelux*, pages 34–41.